Acta Metall. Sin. (Engl. Lett.), 2017, **30**(5), 493–498
DOI 10.1007/s40195-017-0558-7

Tailoring Microstructure and Tribological Properties of Cold Deformed TiZrAlV Alloy by Thermal Treatment

Guo-Sheng Zhang[1] · De-Feng Guo[1,2] · Ming Li[1] · Jing-Tao Li[1,2] · Qian Zhang[1] · Xiao-Hong Li[1] · Xiang-Yi Zhang[1]

Received: 2 December 2016 / Revised: 11 January 2017 / Published online: 3 March 2017

Abstract Microstructure evolution and tribological properties of a new TiZrAlV alloy have been investigated in the present study. Various microstructures, i.e., equiaxed grain structure, dual-phase lamella structure, and heterogeneous lamellar structure, have been successfully prepared, and the effect of the microstructure on tribological properties was explored by means of cold severe plastic deformation combined with subsequent recrystallization annealing and aging treatments. The special heterogeneous lamellar-structured alloy exhibits a high ultimate tensile strength (~1545 MPa), reasonable ductility (~7.9%), and excellent wear resistance as compared with the equiaxed grain-structured and dual-phase lamella-structured alloy. The present study demonstrates an alternative route for enhancing the tribological properties of alloys with heterogeneous lamellar structure.

KEY WORDS: Titanium alloy; Severe plastic deformation; Thermal treatment; Microstructure; Tribological property

1 Introduction

Tribological properties are closely dependent on strength and plasticity. Normally, wear resistance can be enhanced by increasing strength because hard material hinders the press/cut of a friction pair into its surface and decreases its adhesion to the friction pair's surface [1–4]. Simultaneously, high plasticity also contributes to wear resistance by inhibiting brittle fracture formation during sliding wear [5].

Available online at http://link.springer.com/journal/40195

✉ De-Feng Guo
guodf@ysu.edu.cn

✉ Xiang-Yi Zhang
xyzh66@ysu.edu.cn

[1] State Key Laboratory of Metastable Materials Science and Technology, Yanshan University, Qinhuangdao 066004, China

[2] College of Science, Yanshan University, Qinhuangdao 066004, China

To enhance the strength of metals and alloys, thermal–mechanical deformation, e.g., hot rolling, has been widely employed. However, the grain size of thermal–mechanical deformed materials is limited from several to tens of micrometers, which limits the further enhancement of strength of metallic materials. Recently, cold severe plastic deformation (SPD) has been employed to change the microstructure leading to improvement in mechanical properties of metals and alloys [6–8]. By using the combination of cold deformation, e.g., asymmetrical rolling and cryorolling, and subsequent thermal treatments, heterogeneous lamellar structures and multimodal structures have been introduced into Ti, Cu, and Zr [9–11]. By using room temperature rolling and subsequent annealing, and aging, hierarchical structures have been formed in Ti-based alloy [12]. The formation of these heterogeneous structures can be attributed to high cold deformation energy storage permitting high nucleation rates of recrystallization and phase transformation during the thermal treatment, which then produces various microstructures in deformed materials [13]. These heterogeneous-structured

materials exhibited unprecedented mechanical properties, e.g., unusual high strength and ductility [9]. Researchers have attributed these optimized mechanical properties to the back stress effect or complex strain paths in these heterogeneous-structured materials [9, 10]. These results indicate a potential to yield good tribological performance by using cold deformation and subsequent thermal treatment. However, the effect of microstructure of cold deformed materials upon annealing on tribological properties has been rarely explored.

As a new member of the Ti alloy family, TiZrAlV alloy developed from Ti6Al4V alloy shows great potential application in aerospace and aircraft due to its attractive properties, such as the resistance to radiation [14–16]. In the present study, TiZrAlV alloy was used as a model alloy, and the microstructure and tribological properties of cold-rolled TiZrAlV samples after thermal-treated at different conditions were investigated. Microstructural evolution with thermal treatment and the relationship between tribological properties and microstructure were discussed.

2 Experimental Procedure

After solution treatment at 850 °C for 1 h and subsequent water quenching, a nearly single β phase-structured 40.2Ti–51.1Zr–4.5Al–4.2V (wt%) alloy (abbreviated as TiZrAlV below) was attained. The as-quenched TiZrAlV sheets were rolled with a reduction of $\sim$2% per pass at room temperature (RT) to yield a severely deformed sample. An accumulated strain of $\sim$2.65 and a strain rate of $\sim$1.5 s^{-1} were achieved. More experimental details can be found in Ref. [16]. Subsequently, the TiZrAlV sheets subjected to SPD were treated by a three-step thermal treatment in a vacuum furnace. The thermal treatment was composed of a one-step recrystallization annealing and a two-step aging treatment. First, the SPD sample was treated by recrystallization annealing at 675 °C for 10 min (A) to yield an equiaxed β grain structure. Then, the annealed sample was aged at 625 °C for 2 h (B) to precipitate α grains and lamellas in β grains. Finally, the first-step aged sample suffered from the second-step aging at 300 °C for 1.5 h (C) to precipitate α'' lamellas in residual β phase.

To simulate the outer space environment and study the effect of microstructure on the tribological properties of TiZrAlV samples, friction wear tests were performed in vacuum ($p < 10^{-4}$ Pa) using a ball-on-disk GTM-3E tribometer with a load of 4 N. The sample size was 18 mm in diameter and 0.5 mm in thickness. The hardness of the GCr 15 ball with a diameter of 6 mm was 720–780 HV. The rotation diameter and speed were 7 mm and 200 rpm, respectively. Uniaxial tensile tests were performed on the samples with a gauge length of 2.2 mm × 0.35 mm × 5.0 mm at a strain rate of 0.001 s^{-1} using an Instron 5948 Micro-Tester at RT. The tensile direction was parallel to the rolling direction of the samples. More than three times of the friction wear and tensile tests were performed on each sample to ensure reproducible results.

The mass and hardness were measured using an electronic balance and a Shimadzu HMV-2000 Vickers microhardness tester, respectively. The microstructure of samples on the rolling plane and the worn subsurface was characterized by transmission electron microscopy (TEM; JEM-2010). Optical metallography and field emission scanning electron microscopy (FESEM; Hitachi S-4800) were used to examine the morphology of the worn sample surfaces.

3 Results and Discussion

Figure 1 presents the TEM images of SPD TiZrAlV samples after three different thermal treatments. After the annealing at 675 °C for 10 min (Fig. 1a), coarse β grains with an equiaxed grain having an average grain size of $\sim$12 μm were observed. After the first-step aging at 625 °C for 2 h (Fig. 1b), some coarse α lamellas (indicated

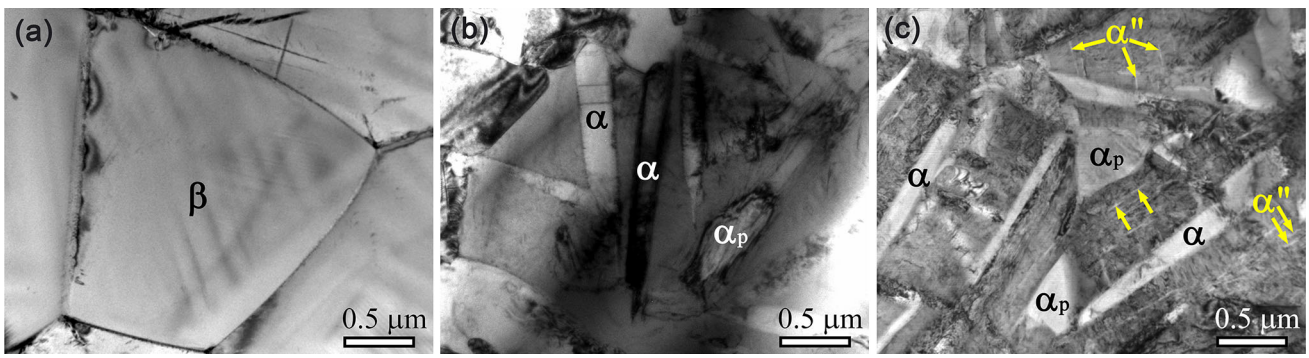

Fig. 1 Bright-field TEM images of the annealed **a**, first- **b**, second-step **c** aged SPD TiZrAlV samples. The equiaxed α grains, α lamellas, and α'' lamellas are indicated by the *symbols* α_p, α, and *yellow arrows*, respectively

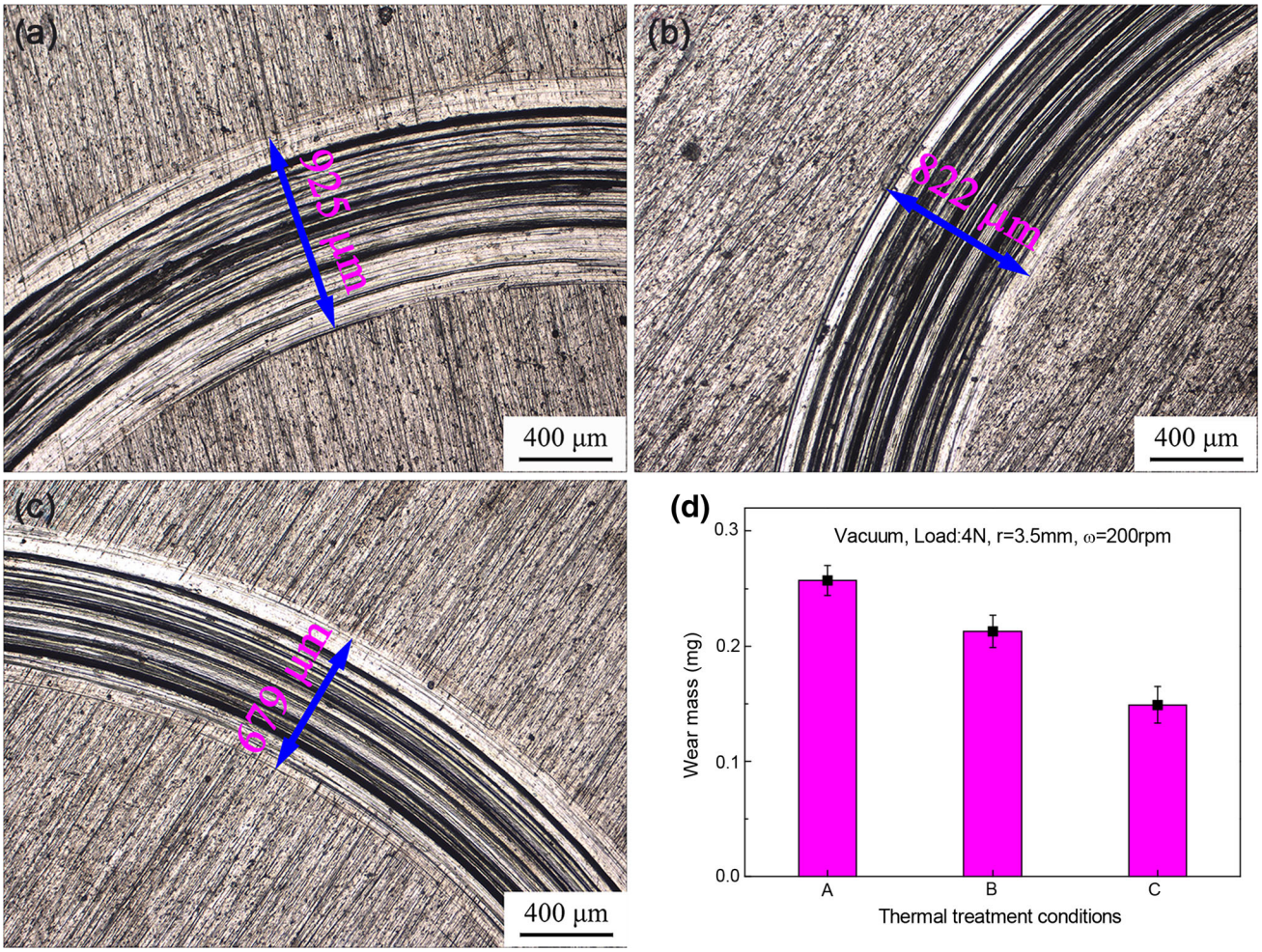

Fig. 2 Metallographic images of the surface morphologies of the annealed **a**, first- **b**, second-step **c** aged SPD TiZrAlV samples after a 6000-cycle friction wear test. The variation in wear mass with the increasing thermal treatment procedure is shown in **d**

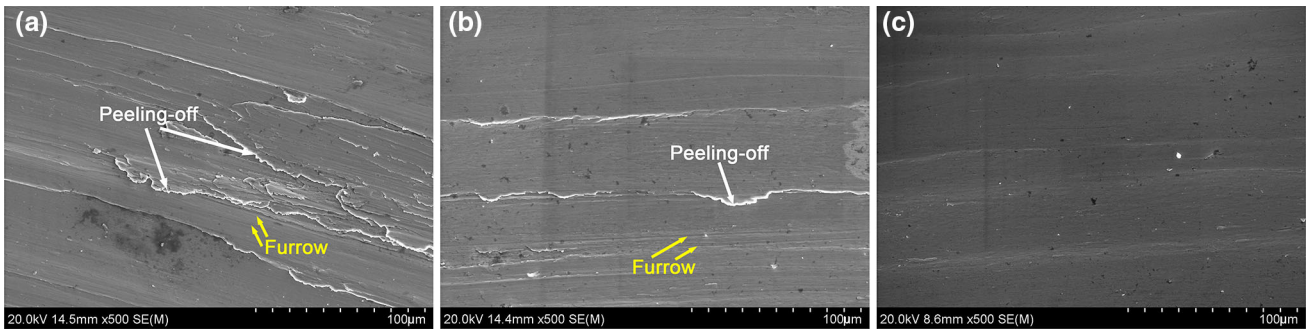

Fig. 3 FESEM images of surface morphologies of annealed **a**, first- **b**, second-step **c** aged SPD TiZrAlV samples after a 6000-cycle friction wear test

by α) and equiaxed α grains (indicated by α_p) appeared in the β primary grains, showing a typical dual-phase lamella structure [15, 17]. After the second-step aging at 300 °C for 1.5 h (Fig. 1c), numerous needle-like α'' lamellas (indicated by yellow arrows), together with some equiaxed α grains, were presented in the residual β phase between α lamellas, demonstrating a heterogeneous lamellar structure [9]. The phase structures of these lamellas and grains were determined by selected area electron diffraction (SAED) analysis [12]. The above TEM observations revealed that the annealing, first- and second-step aging resulted in the formation of equiaxial grained, dual-phase lamella and

heterogeneous lamellar structures in the cold deformed TiZrAlV alloy, respectively.

Figure 2 presents the comparison of tribological properties of SPD TiZrAlV samples after thermal treatments, demonstrating an increase in wear resistance. After a 6000-cycle friction wear test, the widths of the wear track were ~925, ~822, and ~679 μm for the annealed, first- and second-step aged samples (Fig. 2a–c), respectively. And the mass weighing gave a decreased wear mass corresponding to the three different thermal treatment procedures. Both the decreased wear track width and wear mass showed an increase in the wear resistance. Moreover, the increase in wear resistance was also confirmed by SEM observations (Fig. 3a–c). On the wear surface of the annealed SPD sample (Fig. 3a), severe peeling and deep furrows running parallel to the sliding direction were observed, showing severe wear damage. However, for the first-step aged sample (Fig. 3b), slight peeling and shallow furrows were present. After the second-step aging, a smooth surface with shallow furrows was observed on the worn surface (Fig. 3c). The results indicate the fewer and shallower peeling and furrows, the lower wear damage, i.e., the better wear resistance.

To reveal the enhanced wear resistance of SPD TiZrAlV under different thermal treatment procedures, the mechanical properties were evaluated. The tensile engineering stress–strain curves of the SPD samples after thermal treatments are shown in Fig. 4. The annealed sample exhibited a low ultimate tensile strength σ_b of ~987 MPa and a large elongation to failure ε_f of ~21.1% (curve A). After the first-step aging, σ_b increased to ~1140 MPa, whereas ε_f sharply decreased to ~11.9%

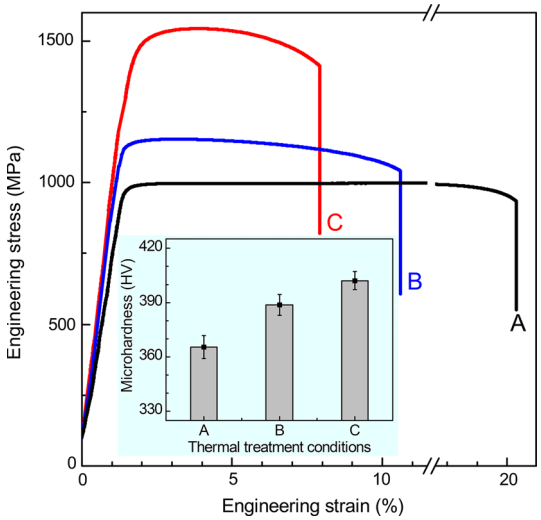

Fig. 4 Engineering tensile stress–strain curves of SPD samples after annealing **a**, first- **b**, second-step **c** aging. The inset shows the Vickers hardness of TiZrAlV samples after annealing, first- and second-step aging treatments

(curve B). After the second-step aging, σ_b sharply increased to ~1545 MPa, whereas ε_f slightly decreased to ~7.9% (curve C). The increase in strength was also confirmed by Vickers hardness measurement, which gave the Vickers hardness of ~365, ~388, and ~402 HV corresponding to the three thermal-treated SPD samples (see the inset in Fig. 4). The low strength and hardness of annealed sample can mainly be attributed to the large amounts of pure soft β phase (Fig. 1a). After the first-step aging, equiaxed α grains and α lamellas were formed in the TiZrAlV samples (Fig. 1b), contributing to the enhanced strength and hardness due to the following two factors. First, the α phase is harder than β phase. Second, the formation of α lamellas resulted in a lot of phase boundaries in the sample, which can be acted as barriers to impede dislocation motion. After the second-step aging, needle-like α'' lamellas precipitated in the residual β phase (Fig. 1c), further suppressing the dislocation motion via increasing phase boundaries. This led to the further enhancement in strength and hardness. The increasing hardness augments wear resistance by weakening the plowing effect [18]. Moreover, poor ductility of high-strength material is detrimental for wear resistance. Normally, a high strength higher than 1500 MPa is always accompanied by a limited ductility (e.g., <5%) [14, 19]. Here, appropriate ductility ($\varepsilon_f = 7.9\%$) of the second-step aged sample is also important in maintaining the high wear resistance via suppressing the brittle fracture of surface material during sliding wear [5].

To further investigate the underlying factors contributing to wear resistance, TEM analysis of the subsurface of worn samples was performed. In the annealed sample (Fig. 5a), dislocations were present in some coarse grains (indicated by the triangles), demonstrating typical hardening results from dislocation pile-up and tangling. The flow stress in the sample was low because of the relatively weak grain boundary strengthening. In the first-step aged sample (Fig. 5b), abundant dislocations appeared in the residual β phase (indicated by the triangles). However, these dislocations are difficult to transit into α lamellas because these α lamellas may still be elastically deformed due to their high yield strength. The heterogeneity in the dual-phase lamella structure produces high back stress as pointed out by Wu et al. [9, 20]. This high back stress together with high grain boundary strengthening resulted in high flow stress in the sample. In the second-step aged sample, besides of dislocation accumulation, some small laths (indicated by the red arrows) appeared in the coarse α lamellas (Fig. 5c, d). The small laths were determined to be α'' phase by SAED patterns (Fig. 5e). The appearance of α'' lath in the interior of α lamellas signified the occurrence of α to α'' martensitic transformation during the friction wear test, which is different from the isothermal transformation

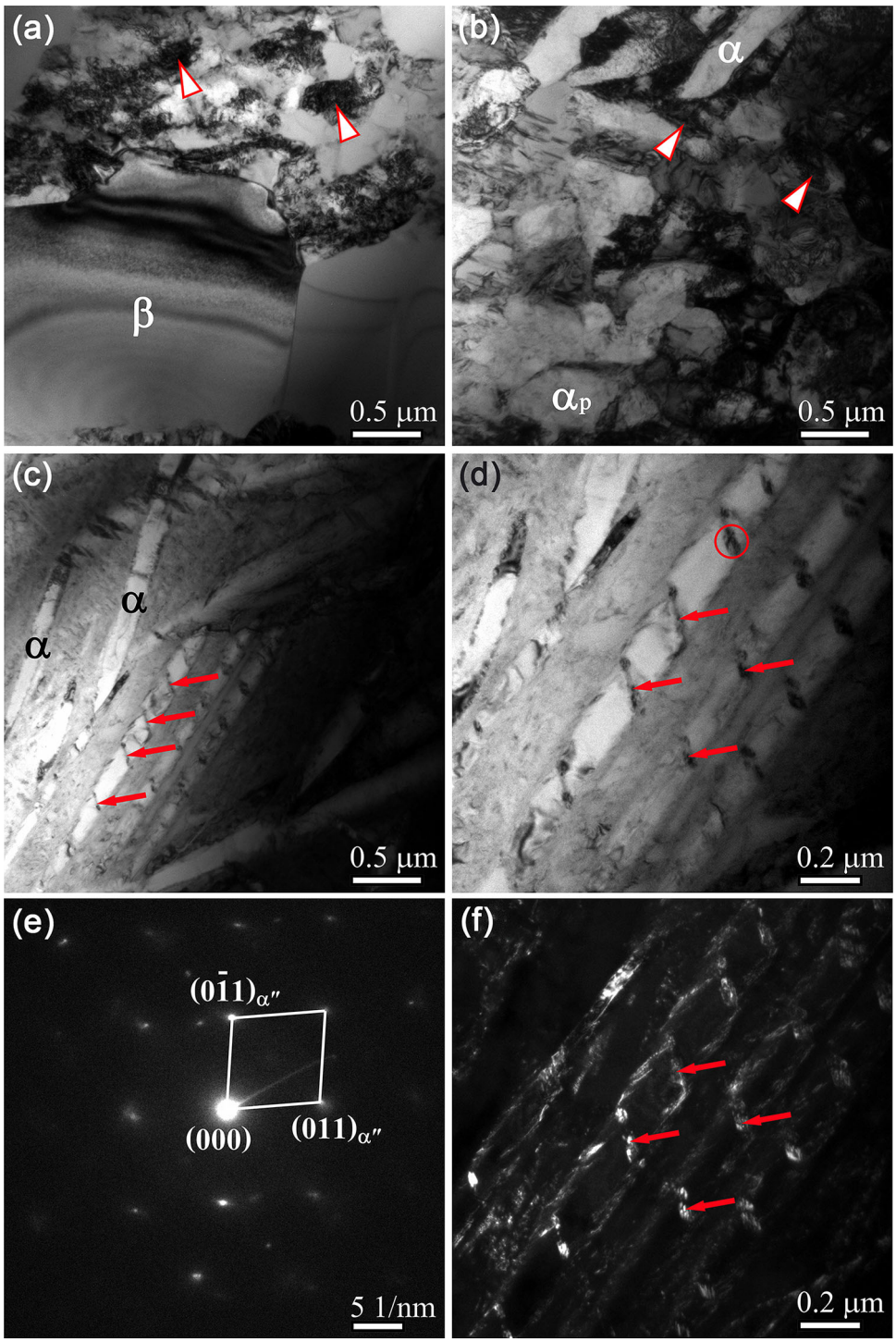

Fig. 5 Subsurface bright-field TEM images of the annealed **a**, first- **b**, second-step **c** aged SPD TiZrAlV samples after friction wear test. **d**, **f** High-magnification bright- and dark-field images of the local area in **c**. **e** SAED pattern is achieved from the encircled region in **d**. Dislocations in **a**, **b**, α'' laths in **c** are indicated with triangles and *red arrows*, respectively

of β to α'' phase during the second-step aging. The latter led to the formation of needle-like α'' phase in residual β phase (Fig. 1c). As a comparison, there is no α'' lath found in the interior of the α lamellas of the first-step aged samples. The phase boundaries in the α lamellas should be increased due to the formation of α'' lath in them. Although α'' phase is softer than α phase, the newly formed α'' laths may still increase the strength and hardness of the TiZrAlV alloy by hindering dislocation motion via the increased phase boundaries, thereby contributing to wear resistance.

Similar wear-induced martensite transformation has not been reported in other Ti alloys. The study on the effect of martensite transformation on wear resistance is currently underway.

One point should be mentioned that many equiaxed grain-structured Ti-based alloys also have been reported to exhibit ultrahigh strength and good ductility. For example, equiaxed grain-structured TiNb alloys were prepared via introducing strengthening phase FeTi or $CoTi_2$ into β-Ti matrix and exhibited excellent mechanical properties, including high strength, good ductility, and high wear resistance [21–25]. Here, an equiaxed grain structure without any precipitates was formed in the annealed TiZrAlV alloy. The equiaxed grain-structured TiZrAlV alloy exhibited a poor wear resistance, which should be attributed to its low strength due to the lack of strengthening phases. Conversely, due to the existence of structural gradient (e.g., α and α'' lamellas in different scales), the second-step aged TiZrAlV exhibits a good combination of high strength, good ductility, and high wear resistance. These results demonstrated that forming a hierarchical structure is an effective way to optimize wear properties of metallic materials.

4 Conclusion

Three different microstructures are formed in a TiZrAlV alloy by employing a combination of cold SPD and different thermal treatments. Compared with the equiaxed grain-structured and dual-phase lamella-structured alloy samples, the TiZrAlV alloy with heterogeneous lamellar structure exhibits an excellent wear resistance. The high wear resistance could be mainly attributed to the combination of high strength and reasonable ductility provided by the heterogeneous lamellar structure. Moreover, the transformation of α to α'' phase during sliding wear also contributed to the enhanced wear resistance. The present study revealed that the heterogeneous structure is promising for high wear resistance and may attract extensive interest for engineering applications.

Acknowledgements The authors gratefully acknowledge the financial support of the National Basic Research Program of China (No. 2010CB731606), the National Natural Science Foundation of China (Nos. 51471144, 51471145, and 51371074), and the research project of the Ministry of Education (No. ZD2016076) of Hebei Province.

References

[1] J.F. Archard, J. Appl. Phys. **24**, 981 (1953)
[2] T. Gloriant, J. Non-Cryst. Solids **316**, 96 (2003)
[3] E. Hornbogen, Wear **33**, 251 (1975)
[4] I. Sevim, I.B. Eryurek, Mater. Des. **27**, 911 (2006)
[5] B. Wang, B. Yao, Z. Han, J. Mater. Sci. Technol. **28**, 871 (2012)
[6] R. Valiev, Nat. Mater. **3**, 511 (2004)
[7] J.C. Lee, H.K. Seok, J.Y. Suh, Acta Mater. **50**, 4005 (2002)
[8] B. Mirzakhani, Y. Payandeh, Mater. Des. **68**, 127 (2015)
[9] X.L. Wu, M.X. Yang, F.P. Yuan, G.L. Wu, Y.J. Wei, X.X. Huang, Y.T. Zhu, Proc. Natl. Acad. Sci. **112**, 14501 (2015)
[10] Y.M. Wang, M.W. Chen, F.H. Zhou, E. Ma, Nature **419**, 912 (2002)
[11] D.F. Guo, M. Li, Y.D. Shi, Z.B. Zhang, H.T. Zhang, X.M. Liu, B.N. Wei, X.Y. Zhang, Mater. Des. **34**, 275 (2012)
[12] Y.D. Shi, M. Li, D.F. Guo, G.S. Zhang, Q. Zhang, X.H. Li, X.Y. Zhang, Mater. Sci. Eng. A **615**, 464 (2014)
[13] S.Q. Deng, A. Godfrey, W. Liu, Acta Metall. Sin. (Engl. Lett.) **29**, 313 (2016)
[14] S.X. Liang, M.Z. Ma, R. Jing, Y.K. Zhou, Q. Jing, R.P. Liu, Mater. Sci. Eng. A **539**, 42 (2012)
[15] Z.B. Zhang, G.S. Zhang, D.F. Guo, M. Li, Y.D. Shi, X.H. Li, X.Y. Zhang, Mater. Lett. **131**, 240 (2014)
[16] D.F. Guo, X.H. Li, M. Li, Y.D. Shi, G.S. Zhang, K. Sato, Z.J. Zhang, X.Y. Zhang, Scr. Mater. **108**, 64 (2015)
[17] H.C. Kou, H.L. Zhang, Y.D. Chu, D. Huang, H. Nan, J.S. Li, Acta Metall. Sin. (Engl. Lett.) **28**, 505 (2015)
[18] D.H. Jeong, F. Gonzalez, G. Palumbo, K.T. Aust, U. Erb, Scr. Mater. **44**, 493 (2001)
[19] I.P. Semenova, G.I. Raab, L.R. Saitova, R.Z. Valive, Mater. Sci. Eng. A **387**, 805 (2004)
[20] M.X. Yang, Y. Pan, F.P. Yuan, Y.T. Zhu, X.L. Wu, Mater. Res. Lett. **4**, 145 (2016)
[21] C. Yang, L.H. Liu, Q.R. Cheng, D.D. You, Y.Y. Li, Mater. Sci. Eng. A **580**, 397 (2013)
[22] L.H. Liu, C. Yang, F. Wang, S.G. Qu, X.Q. Li, W.W. Zhang, Y.Y. LI, L.C. Zhang, Mater. Des. **79**, 1 (2015)
[23] D.S. Zhou, F. Qiu, H.Y. Wang, Q.C. Jiang, Acta Metall. Sin. (Engl. Lett.) **27**, 798 (2014)
[24] L.H. Liu, C. Yang, L.M. Kang, Y. Long, Z.Y. Xiao, P.J. Li, L.C. Zhang, Mater. Sci. Eng. A **650**, 171 (2016)
[25] L.M. Zou, L.J. Zhou, C. Yang, S.G. Qu, Y.Y. Li, J. Mater. Res. **29**, 902 (2014)